Journal of Information Systems Engineering and Management
2024, 9(4s)
e-ISSN: 2468-4376
https://www.jisem-journal.com/

Research Article

Hybrid Stability Index based Optimal TCSC Placement with ALO for Enhanced Power System Performance

J. Ayyappa[1*], Dr. N. Jayakumar[2], Dr. A. Srinivasa Reddy [3]
[*1]*Research Scholar, Department of Electrical and Electronics Engineering, Annamalai University, Annamalai Nagar, Chidambaram, Tamil Nadu, India*
and
Assistant Professor, Department of Electrical and Electronics Engineering, Sir C R Reddy College of Engineering, Eluru, Andhra Pradesh, India
Email: ayyappacrr@gmail.com
[2]*Assistant Professor, (Deputed from Annamalai University) Lecturer, Dept. of EEE Government Polytechnic College, Ariyalur. Tamil Nadu, India.*
Email: jayakumar_382@yahoo.co. in
[3] *Professor & HOD, EEE Dept., Sir C. R. Reddy College of Engineering, Eluru, India.*

ARTICLE INFO

Received: 13 Oct 2024

Revised: 27 Nov 2024

Accepted: 25 Dec 2024

ABSTRACT

Driven by privatisation, the changing terrain of the electricity sector requires the best use of the resources at hand to attain operational dependability as well as economic efficiency. Solving these difficulties depends much on optimal power flow (OPF). Maintaining system security depends on guarantees of power system stability under both normal and contingency conditions at the same time. Particularly the Thyristor Controlled Series Compensator (TCSC), the combination of Flexible AC Transmission System (FACTS) devices provide a good way to improve system stability and reduce possible contingencies. This work suggests a new method for the optimal location of TCSC based on a hybrid stability index (HSI), which jointly identifies the most important lines under stressed system conditions by aggregating the Fast Voltage Stability Index (FVSI) with the Line Utilization Factor (LUF). In parallel, seeking to improve system performance, the Ant Lion Optimizer (ALO) method is used for best generator tuning. We develop a multi-objective optimization framework to reduce transmission line losses, active power production cost, and voltage deviation. Extensive simulations on the IEEE 30-bus test system confirm the validity of the suggested approach. Its performance also is compared with the Harmony Search (HS) method. The results verify that in terms of solution quality and contingency management capacity the combined HSI-based TCSC placement and ALO-based generator tuning method beats the HS algorithm.

Keywords: Optimal Power Flow (OPF), Ant Lion Optimizer (ALO), Thyristor Controlled Series Compensator (TCSC), Hybrid Stability Index (HSI), Line Utilization Factor (LUF), Fast Voltage Stability Index (FVSI), Harmony Search (HS), Power System Contingency Management, FACTS Devices, Voltage Stability.

1. INTRODUCTION

The difficulties related to the operations and planning of electricity systems have gotten more complicated as they keep changing under the effect of privatisation and deregulation. More intelligent tools will help to improve system dependability and long-term stability as well as economic efficiency. Among these instruments, OPF has become a pillar as it allows one to reconcile technical grid limits with minimising generating costs, lowering of power losses, and preservation of voltage levels [1], [2]. The broad integration of renewable energy sources and the changing character of demand create extra pressure on the modern grid, thus system stability under both normal operations and unanticipated contingency becomes a major issue [3], [4]. Utilities are so depending more and more on FACTS technology in reaction. Particularly technologies like the TCSC have showed considerable promise in improving voltage profiles, increasing power transfer capability, and grid assistance during disturbances [5], [6].

Journal of Information Systems Engineering and Management
2024, 9(4s)
e-ISSN: 2468-4376
https://www.jisem-journal.com/

Research Article

For FACTS devices like TCSC, however, their placement and setup must be precisely optimized if they are to yield best results. From more complex approaches like mixed-integer programming to more traditional methods like linear and nonlinear programming, researchers have addressed this problem using a range of approaches [7], [8]. Because they can effectively solve difficult, non-linear, multimodal problems over time, metaheuristic algorithms have become rather popular For this aim [9], [10], [11], [12], [13], [14], [15] have been extensively applied techniques like Genetic Algorithms (GA), Particle Swarm Optimization (PSO), Differential Evolution (DE), Ant Colony Optimization (ACO), Simulated Annealing (SA), and Harmony Search (HS). Particularly appreciated for its balance between exploration and exploitation, which lets it identify optimal solutions more consistently and rapidly in large-scale OPF applications, the Ant Lion Optimizer (ALO) has become a strong alternative in recent years [16], [17]. While efficiently managing several objectives and system uncertainties studies have demonstrated that ALO can successfully reduce generating costs and reactive power losses [18], [19]. Further increasing accuracy and robustness, even greater results have been seen when ALO is hybridised with other intelligent techniques as fuzzy logic systems, neural networks, or local search upgrades [20] [21]. Concurrent with these optimization initiatives, voltage stability has attracted significant attention particularly in systems under stress or vulnerable to interruptions. To assess how near a system is to voltage collapse [22], [23], [24], several indices like the FVSI, Line Stability Index and LUF have been developed. Still, none one index can present a whole picture. Therefore, this work suggests a HIS combining the advantages of FVSI and LUF to find the most sensitive transmission lines and direct the best location of TCSC devices [25].

Contingency analysis is still therefore a crucial component of preserving grid security. The norm is still traditional N-1 analysis, which lets operators forecast component failures and system problems. Which contingency causes the most risk is ranked using complementary indices such the Performance Index (PI), L-index, and other combinatory techniques [26], [27], [28]. These instruments greatly increase the grid's resilience against faults and outages when combined with modern OPF models and FACTS-based solutions [29], [30]. Considering all this, this work presents an integrated OPF framework supported by conventional contingency analysis methods that combines the ALO-based generator tuning and HSI-guided TCSC allocation. An IEEE-30-bus test system is used for validation of the framework against the Harmony Search method. Results show that the suggested method presents better performance in terms of cost savings, voltage control, and contingency handling so giving a strong solution for contemporary, dynamic, and safe power system operations.

2. MODELLING OF TCSC

The primary TCSC system put forth by Vithayathil and the rest in 1986 was a technique related to “rapid adjustment of network impedance”. In addition to controlling the line power moving capacity, the TCSC goes on to enhance the system firmness. The primary unit of TCSC is displayed through Fig.1. It makes up a series recompensing capacitor that is shunted via the thyristor-controlled reactor. Thyristor incorporation in TCSC module facilitates smooth and steadier control of reactance against system criteria differences. In case of a massive power system, TCSC execution needs numerous similar primary compensators in order to get linked in series for acquiring required voltage rating as well as operating traits. It has been modelled in the form of a controllable reactance, gets included in series with the transmission line to fine-tune line impedance and thus controls the power flow.

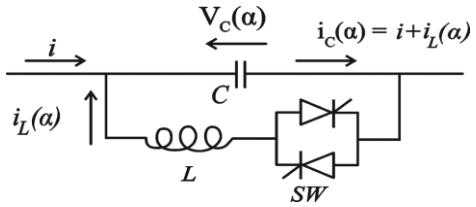

Fig.1: Basic TCSC model

Here, there is a straight fine-tuning of the reactance of the transmission line with the use of TCSC. The TCSC is modelled as varied impedance and its rating relies on the reactance of the transmission line where the TCSC is situated. From Fig.2, the impedance equations are written as in equations 1 to 3.

Journal of Information Systems Engineering and Management
2024, 9(4s)
e-ISSN: 2468-4376
https://www.jisem-journal.com/

Research Article

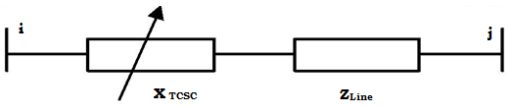

Fig.2: Block diagram of TCSC

$$Z_{ij} = R_{ij} + X_{ij} \quad (1)$$

$$Z_{line} = R_{line} + X_{line} \quad (2)$$

$$X_{ij} = X_{line} + X_{TCSC} \quad (3)$$

Where X_{TCSC} is reactance of TCSC, without over compensation, the working range of the TCSC is selected to lie within -0.8$X_{line}$and 0.6X_{line}. The transfer admittance matrix of the TCSC is given by

$$\begin{bmatrix} I_i \\ I_j \end{bmatrix} = \begin{bmatrix} jB_{ii} & jB_{ij} \\ jB_{ji} & jB_{jj} \end{bmatrix} \begin{bmatrix} Vi \\ V_j \end{bmatrix} \quad (4)$$

For capacitive operation, equations are given in (5) and (6)

$$B_{ii} = B_{jj} = \frac{1}{X_{TCSC}} \quad (5)$$

$$B_{ij} = B_{ji} = -\frac{1}{X_{TCSC}} \quad (6)$$

For inductive operation, the signs are inverted or reversed.

The active and reactive power equations at bus k are:

$$P_i = V_i V_j B_{ij} \sin(\theta_i - \theta_j) \quad (7)$$

$$Q_i = -V_i^2 B_{ii} - V_i V_j B_{ij} \cos(\theta_i - \theta_j) \quad (8)$$

When the series reactance controls the amount of active power flowing from bus i to bus j the change in reactance of TCSC is:

$$\Delta X_{TCSC} = X_{TCSC}^{i} - X_{TCSC}^{(i-1)} \quad (9)$$

Based on optimization rules, the state variable X_{TCSC} of the series controller is updated.

3. PROPOSED HYBRID STABILITY INDEX (HSI) FOR OPTIMAL PLACEMENT OF TCSC

HSI is a combination of line loading index and voltage stability index. It gives an accurate measure of the stress on a bus. Thus, accurately defining its weakness with respect to others.

A combined index is formulated using LUF and FVSI indices as given in equation (10)

$$HSI = Z1 \times S1 + Z2 \times S2 \quad (10)$$

Where, Z_1 and Z_2 are the weighting factors.

$S_1$is the Line Utilization Factor is an index used for determining the congestion of the transmission lines.

LUF is given by equation (11)

$$S1 = \frac{MVAij}{MVAij^{max}} \quad (11)$$

MVAij (max): Maximum MVA rating of the line between bus i and busj.

MVAij : Actual MVA rating of the line between bus i and bus j.

Journal of Information Systems Engineering and Management
2024, 9(4s)
e-ISSN: 2468-4376
https://www.jisem-journal.com/

Research Article

LUF gives an estimate of the percentage of line being utilized.

Fast Voltage Stability Index Factor (FVSI) calculates the voltage stability of a given bus under any loading conditions. It is defined as follows

S_2 is the Fast Voltage Stability Index (FVSI) given by equation (12)

$$S2 = 4\frac{Z^2 Qj}{Vi^2 X} \quad (12)$$

Where, Z is the impedance of line.

X is the line reactance.

V_i is the voltage at the sending end.

Q_j is the reactive power at the receiving end.

4. PROBLEM FORMULATION:

For the best generator tuning, a multi-objective function that considers the fuel cost, real power loss, and voltage variation was employed.

$$\text{Min } F = \text{Min } (W1 * F1 + W2 * F2 + W3 * F3) \quad (13)$$

Where, F1 is the Fuel cost given by

$$F1 = \min\left(\sum_{i=1}^{ng}(a_i + b_i P_{Gi} + C_i P_{Gi}^2)\right) \quad (14)$$

The number of generators in the power system is represented by Ng and the fuel cost coefficients are a, b, and c. Table.1 lists the values of the coefficients for the several generators.

In this case, there are ntl transmission lines and Sjk is the total complex power flowing from bus j to bus k in line i, where F2 denotes the voltage variance.

$$F2 = \min(VD) = min\left(\sum_{k=1}^{Nbus}\left(V_K - S_k^{ref}\right)^2\right) \quad (15)$$

The reference value of the voltage magnitude at bus is V_k^{ref}, whereas the actual voltage magnitude at bus k is V_k.

The true power loss is F3.

$$F3 = min\left(\sum_{i=1}^{ntl} real\left(S_{jk}^i + S_{kj}^i\right)\right) \quad (16)$$

Equality constraints:

Power Balance Constraint

$$\sum_{i=1}^{N} P_{Gi} = \sum_{i=1}^{N} P_{Di} + P_L \quad (17)$$

$$\sum_{i=1}^{N} Q_{Gi} = \sum_{i=1}^{N} Q_{Di} + Q_L \quad (18)$$

Where i=1, 2, 3... N and N = no. of. PL indicates the active power loss of the system, Q_L is the total reactive power loss, P_{Gi} is the active power generated at bus i, Q_{Gi} is the reactive power generated at bus i, P_{Di} is the power demand at bus i, Q_{Di} is the power demand at bus i, and N is the number of buses.

Table.1: Fuel Cost Calculation Values for a, b, and c

Generator bus no	a (p.u)	b (p.u)	c (p.u)
1	0.005	2.45	105
2	0.005	3.51	44.1
5	0.005	3.89	40.6

Journal of Information Systems Engineering and Management
2024, 9(4s)
e-ISSN: 2468-4376
https://www.jisem-journal.com/

Research Article

8	0.005	3.25	0
11	0.005	3	0
13	0.005	2.45	105

Inequality constraints:

Voltage balance constraint

$$V_{Gi}^{\min} \le V_{Gi} \le V_{Gi}^{\max} \quad (19)$$

Where Gi=1, 2, 3... ng and ng = number of Generator buses.

Real power generation limit:

$$P_{Gi}^{\min} \le P_{Gi} \le P_{Gi}^{\max} \quad (20)$$

Where, Gi=1, 2, 3... ng

where ng is the number of generator buses.

Reactive Power generation limits:

$$Q_{Gi}^{\min} \le Q_{Gi} \le Q_{Gi}^{\max} \quad (21)$$

Ant Lion Optimizer

ALO is a metaheuristic inspired by antlion hunting behavior, where ants perform constrained random walks within dynamically shrinking boundaries around selected antlions, enhancing convergence through elite guidance and adaptive search boundaries. The equation (22) normalizes the ant's position within shrinking bounds influenced by a selected antlion to balance exploration and exploitation during optimization.

$$X_k^t = \frac{(X_k^t - a_k) \times (d_k^t - c_k^t)}{b_k - a_k} + c_k^t \quad (22)$$

The equations update the lower (c_k^n) and upper (d_k^n) bounds of the ant's search space based on the position of the selected antlion and the shrinking vectors c^n and d^n . The equations (25) and (26) reduce the shrinking vectors c^n and d^n over time, where I is the shrinking constant, to intensify the search around promising solutions. The values c^n and d^n represent the minimum and maximum bounds of all variables at the nth iteration, while the constant I is defined as $I = 10^{\frac{w.n}{N}}$ where n is the current iteration, N is the total number of iterations, and w is a constant controlling the shrinking rate.

$$c_k^n = Antlion_k^n + c^n \quad (23)$$

$$d_k^n = Antlion_k^n + d^n \quad (24)$$

$$c^n = \frac{c^n}{I} \quad (25)$$

$$d^n = \frac{d^n}{I} \quad (26)$$

5. RESULTS AND DISCUSSION

Proposed Approach

This work proposes a structured four-step optimization model that utilizes the Ant Lion Optimizer (ALO) in conjunction with TCSC placement guided by a Hybrid Stability Index (HSI). The goal is to minimize fuel cost, active power losses, and voltage variations, thereby enhancing system performance and voltage stability under both normal and contingency conditions.

Journal of Information Systems Engineering and Management
2024, 9(4s)
e-ISSN: 2468-4376
https://www.jisem-journal.com/

Research Article

First Step: Initially, the OPF problem is solved under normal operating conditions using the ALO algorithm. The objectives are to ensure economic operation by minimizing both real power losses and total generation cost, while also improving voltage profiles across the system. All operational and security constraints are strictly observed, and generator outputs are maintained within their permissible limits. ALO is implemented to determine optimal generator settings, and its performance is evaluated in terms of cost, losses, and voltage deviations.

Second Step: In the second phase, TCSC placement is carried out based on the proposed HSI, which combines the LUF and FVSI. This combined index accurately pinpoints lines that are most prone to instability. The transmission line with the highest HSI value is selected as the optimal TCSC location. OPF is then re-run using the ALO algorithm with TCSC integrated into the selected line. The outcomes are compared with the results from the first step to assess the effectiveness of TCSC in improving system voltage stability and reducing system stress.

Third Step: The third step involves contingency analysis and generator reallocation. An N-1 contingency study is performed to evaluate the system's response to the loss of any single transmission line. Each contingency is analyzed using a severity index to determine the most critical scenario. For the most severe contingency, the OPF problem is solved again with re-optimized generator settings using the ALO algorithm. The reallocation aims to support voltage profiles and reduce real power losses under the stressed condition.

Fourth Step: In the final step, re-optimization is performed under the selected contingency scenario, now incorporating TCSC placement. The HSI is recalculated to identify the most vulnerable line under fault conditions. A TCSC is installed at this location to counteract voltage instability and alleviate line congestion. The ALO algorithm is used once more to solve the OPF problem considering both generator reallocation and TCSC. The resulting performance metrics are compared to those from the previous steps, highlighting the overall enhancement achieved and demonstrating the robustness and efficiency of the proposed ALO-TCSC-based optimization strategy under severe system disturbances.

5.1 OPF for Normal Condition (Without Contingency)

Table.2: Non-Dominated Solutions for Fuel Cost, Voltage Deviation, and Transmission Losses.

Set	W_1 (FC)	W_2 (VD)	W_3 (TL)	F Value
1	0.15	0.1	0.75	212.1378
2	0.22	0.1	0.68	306.2311
3	0.26	0.09	0.65	360.0987
4	0.295	0.105	0.6	406.9953
5	0.33	0.09	0.58	454.192
6	0.385	0.08	0.535	528.2226

Set 1 from Table.2 is considered the most suitable operating point for the power system optimization based on the given objectives. In this set, the weight distribution prioritizes the minimization of transmission losses with a dominant weight of $W_3 = 0.75$, while assigning $W_1 = 0.15$ to fuel cost and $W_2 = 0.1$ to voltage deviation. This combination yields the lowest total fitness value of 212.1378, indicating an optimal balance with minimal losses and acceptable levels of fuel cost and voltage variation. By emphasizing transmission losses, Set 1 supports system efficiency and reliability, which are critical under both normal and contingency conditions. Although it gives less weight to fuel cost and voltage deviation, the resulting solution still satisfies all operational constraints and maintains voltage stability within permissible limits. Therefore, Set 1 is selected for further stages of analysis and serves as the reference case for evaluating the performance enhancements achieved by TCSC placement and contingency management.

Journal of Information Systems Engineering and Management
2024, 9(4s)
e-ISSN: 2468-4376
https://www.jisem-journal.com/

Research Article

Table.3: All lines HSI values in the IEEE 30-Bus System Using the HS Algorithm

Rank	Line Connected		LUF	FVSI	HSI	Rank	Line Connected		LUF	FVSI	HSI
	From bus	To bus					From bus	To bus			
1	9	10	0.2307	0.1379	0.1843	17	10	17	0.0423	0.0304	0.03635
2	3	4	0.3012	0.0409	0.17105	18	10	22	0.0377	0.0352	0.03645
3	4	6	0.2832	0.0369	0.16005	19	27	29	0.0308	0.0373	0.03405
4	4	12	0.144	0.1508	0.1474	20	25	27	0.0228	0.0429	0.03285
5	6	7	0.2064	0.0685	0.13745	21	12	14	0.0376	0.0194	0.0285
6	28	27	0.0931	0.1198	0.10645	22	19	20	0.0367	0.0151	0.0259
7	10	21	0.1195	0.0601	0.0898	23	12	16	0.0364	0.0047	0.02055
8	6	10	0.0614	0.0986	0.08	24	23	24	0.0129	0.0245	0.0187
9	12	15	0.0887	0.0219	0.0553	25	15	18	0.0296	0.0036	0.0166
10	6	28	0.078	0.0287	0.05335	26	16	17	0.0194	0.0123	0.01585
11	6	9	0.0694	0.0367	0.05305	27	29	30	0.0173	0.0144	0.01585
12	10	20	0.0494	0.0529	0.05115	28	24	25	0.0033	0.0192	0.01125
13	12	13	0.0986	0.0002	0.0493	29	15	23	0.0205	0.0001	0.01025
14	22	24	0.0371	0.0485	0.0428	30	21	23	0.0164	0.0033	0.00985
15	27	30	0.0352	0.0485	0.04185	31	18	19	0.0134	0.0026	0.008
16	25	26	0.0199	0.0606	0.04025	32	14	15	0.0054	0.0021	0.00375

Table.3 presents the HSI values computed for each transmission line in the IEEE 30-bus system. These values are derived using the HS algorithm, which optimally combines two important indicators: the LUF and the FVSI. The HSI, calculated as a weighted combination of LUF and FVSI, quantifies the stress on each line, identifying how critical or vulnerable each one is in terms of power flow and voltage stability. The table is sorted by HSI ranking, with Rank 1 assigned to the line with the highest HSI value, indicating it is the most stressed and hence the most suitable candidate for compensation via TCSC. The line between Bus 9 and Bus 10 has the highest HSI value of 0.1843, making it the top priority for stability improvement. Similarly, the lines from Bus 3 to 4 and from Bus 4 to 6 follow as the next critical lines with HSI values of 0.17105 and 0.16005, respectively.

As we move down the table, the HSI values gradually decrease, indicating lesser stress and congestion. For instance, lines ranked from 25 to 32 have significantly lower HSI values, with the lowest being 0.00375 for the line between Bus 14 and Bus 15. These lines are relatively stable and not immediate priorities for compensation or reinforcement. Overall, this ranking helps in prioritizing the placement of TCSC devices to enhance system reliability, mitigate congestion, and improve voltage stability. The Harmony Search algorithm ensures that the selection of these critical lines is based on a balanced and optimized evaluation of both real power flow stress and voltage stability conditions.

Table.4 presents the HSI values for all transmission lines in the IEEE 30-bus system, calculated using the ALO algorithm. The HSI is a combined measure that incorporates the LUF and the FVSI, providing a comprehensive assessment of each transmission line's performance in terms of power flow stress and voltage stability. This combined

Journal of Information Systems Engineering and Management
2024, 9(4s)
e-ISSN: 2468-4376
https://www.jisem-journal.com/

Research Article

index helps to identify the most critical lines in the grid that may require additional support to enhance overall stability. The lines are ranked based on their HSI values, with the most critical lines listed at the top. For instance, the line between Bus 9 and Bus 10 has the highest HSI value of 0.1868, making it the top candidate for the installation of a TCSC. This line is experiencing significant congestion and voltage instability, and a TCSC here would help alleviate these issues. Similarly, the line between Bus 3 and Bus 4, with an HSI of 0.17355, and the line between Bus 4 and Bus 6, with an HSI of 0.16255, also show high stress levels and are good candidates for TCSC installation. These lines, with their high HSI values, are more likely to benefit from such devices, which would help mitigate congestion and improve voltage stability.

Table.4: All lines HSI values in the IEEE 30-Bus System Using the ALO Algorithm

Rank	Line Connected		LUF	FVSI	HSI	Rank	Line Connected		LUF	FVSI	HSI
	From bus	To bus					From bus	To bus			
1	9	10	0.2332	0.1404	0.1868	17	10	17	0.0448	0.0329	0.03885
2	3	4	0.3037	0.0434	0.17355	18	10	22	0.0402	0.0377	0.03895
3	4	6	0.2857	0.0394	0.16255	19	27	29	0.0333	0.0398	0.03655
4	4	12	0.1465	0.1533	0.1499	20	25	27	0.0253	0.0454	0.03535
5	6	7	0.2089	0.071	0.13995	21	12	14	0.0401	0.0219	0.031
6	28	27	0.0956	0.1223	0.10895	22	19	20	0.0392	0.0176	0.0284
7	10	21	0.122	0.0626	0.0923	23	12	16	0.0389	0.0072	0.02305
8	6	10	0.0639	0.1011	0.0825	24	23	24	0.0154	0.027	0.0212
9	12	15	0.0912	0.0244	0.0578	25	15	18	0.0321	0.0061	0.0191
10	6	28	0.0805	0.0312	0.05585	26	16	17	0.0219	0.0148	0.01835
11	6	9	0.0719	0.0392	0.05555	27	29	30	0.0198	0.0169	0.01835
12	10	20	0.0519	0.0554	0.05365	28	24	25	0.0058	0.0217	0.01375
13	12	13	0.1011	0.0027	0.0519	29	15	23	0.023	0.0026	0.0128
14	22	24	0.0396	0.051	0.0453	30	21	23	0.0189	0.0058	0.01235
15	27	30	0.0377	0.051	0.04435	31	18	19	0.0159	0.0051	0.0105
16	25	26	0.0224	0.0631	0.04275	32	14	15	0.0079	0.0046	0.00625

In contrast, lines with lower HSI values, such as the line between Bus 21 and Bus 23 (HSI = 0.01235) and the line between Bus 14 and Bus 15 (HSI = 0.00625), are less critical and may not require immediate TCSC installation. These lines exhibit relatively low stress, indicating that they do not pose as significant a risk to the grid's stability. Thus, the HSI values in Table.4 are instrumental in determining the optimal locations for installing TCSC devices, focusing on the lines that experience the highest levels of stress due to line utilization and voltage instability. The ALO algorithm's ability to accurately rank these lines helps in making informed decisions regarding system stability improvements.

The results presented in Table.5 highlight the optimization performance of the HS and ALO methods with and without the inclusion of TCSC. Both methods successfully reduce the total generation when TCSC is applied, indicating the effectiveness of TCSC in optimizing power flow and enhancing system stability. However, ALO

Journal of Information Systems Engineering and Management
2024, 9(4s)
e-ISSN: 2468-4376
https://www.jisem-journal.com/

Research Article

outperforms HS in terms of total generation, with a lower total generation of 287.87 MW when TCSC is included, compared to the 294.58 MW achieved by HS. This suggests that ALO provides a more balanced and efficient distribution of power generation across the system. Additionally, the optimized generator outputs for ALO show better convergence, particularly for generators PG1 and PG8, with smoother adjustments observed compared to HS. This indicates that ALO is more capable of optimizing the generation at each bus while maintaining system constraints. The TCSC parameters, including Ptcsc, Qtcsc, and X, are also more accurately tuned in ALO, further enhancing the system's performance. In conclusion, ALO demonstrates a superior optimization capability compared to HS, especially when TCSC is utilized. ALO achieves a more efficient power distribution, lower total generation, and finer tuning of generator outputs, making it a more effective approach for power system optimization in comparison to the HS method.

Table.5: Optimized Generator Outputs and Total Generation for HS and ALO Methods With and Without TCSC

Method	PG1 (MW)	PG2 (MW)	PG5 (MW)	PG8 (MW)	PG11 (MW)	PG13 (MW)	Total Generation (MW)	TCSC Rating (P.U)
HS without TCSC	137.4123	33.3926	30.0535	43.7988	44.8213	10	299.4785	---------
HS with TCSC at Line No 9-10	133.9512	33.3918	29.3027	44.4495	43.4897	10	294.5849	P_{tcsc}=0.4642 Q_{tcsc}=0.0114 X=0.02
ALO without TCSC	135.3714	20.3396	24.8427	23.9887	80.5158	9.852	294.9102	---------
ALO with TCSC at Line No 9-10	132.1793	20.1007	25.4235	22.3394	77.8227	10	287.8656	P_{tcsc}=0.4632 Q_{tcsc}=0.0113 X=0.02

Table.6: Power Parameters Comparison of HS and ALO Methods With and Without TCSC

Parameter	HS without TCSC	HS with TCSC at Line No 9-10	ALO without TCSC	ALO with TCSC at Line No 9-10
Total Real Power (MW)	299.4785	294.5849	294.9102	287.8656
Real Power Loss (MW)	16.0785	11.1849	11.5102	4.4656
Reactive Power Loss (MVAR)	34.45	14.75	18.78	11.87
Voltage Deviation (p.u.)	1.8507	0.5327	1.5013	0.5122
Fuel Cost ($/hr)	1361.9	1278.5	1355.7	1262.2

Table.6 compares the performance of the HS and ALO methods, both with and without the inclusion of TCSC, by evaluating several key power system parameters. The results indicate that the ALO method outperforms the HS method across all parameters when TCSC is implemented. For total real power generation, ALO with TCSC achieves

Journal of Information Systems Engineering and Management
2024, 9(4s)
e-ISSN: 2468-4376
https://www.jisem-journal.com/

Research Article

the lowest generation (287.87 MW) compared to HS with TCSC (294.58 MW), showing ALO's ability to optimize power generation more efficiently. When it comes to real power loss, ALO with TCSC shows a significant reduction, with a loss of only 4.47 MW, whereas HS with TCSC results in 11.18 MW, highlighting ALO's superior performance in minimizing transmission losses. Similarly, reactive power losses are lower with ALO, at 11.87 MVAR, compared to HS with TCSC at 14.75 MVAR, further demonstrating ALO's advantage in reducing both real and reactive losses. The voltage deviation improves significantly with TCSC in both methods, but ALO with TCSC provides the best performance at 0.5122 p.u., slightly outperforming HS with TCSC (0.5327 p.u.). Finally, the fuel cost is reduced in both methods when TCSC is applied, with ALO with TCSC achieving the lowest fuel cost of $1262.2 per hour, compared to $1278.5 per hour for HS with TCSC. Overall, ALO consistently delivers better results than HS, especially with the incorporation of TCSC, demonstrating its superior capability in optimizing power system operations.

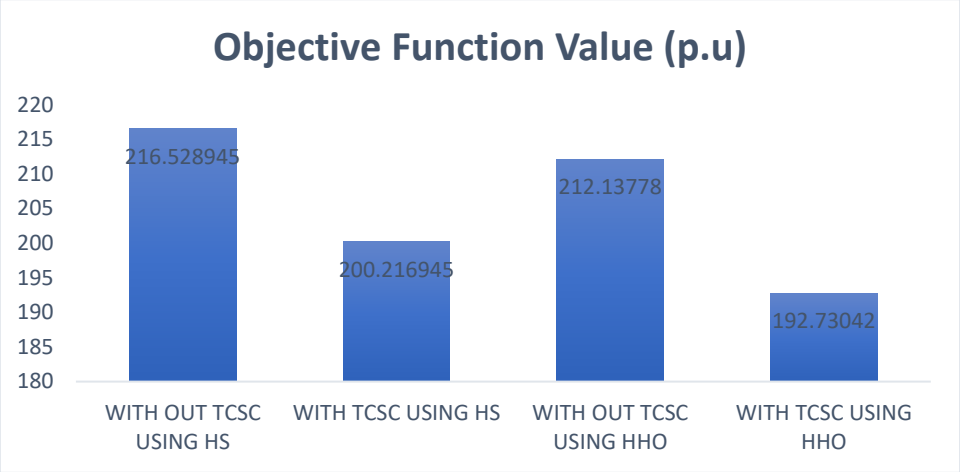

Figure.3: Objective Function (F) Comparison for HS and ALO Algorithms with and Without SVC

The objective function values for both the HS and ALO methods, with and without TCSC, are presented in the Fig.3. For the HS method, the objective function value without TCSC is 216.53 p.u., which decreases to 200.22 p.u. when TCSC is included, indicating an improvement in the system's performance with TCSC. Similarly, for the ALO method, the objective function value without TCSC is 212.14 p.u., and with TCSC, it reduces further to 192.73 p.u. This shows that the ALO method achieves a better overall objective function value, both with and without TCSC, compared to the HS method. The inclusion of TCSC helps improve the optimization process, reducing the objective function value in both methods, with ALO demonstrating a more significant reduction, which indicates its superior ability to optimize system performance.

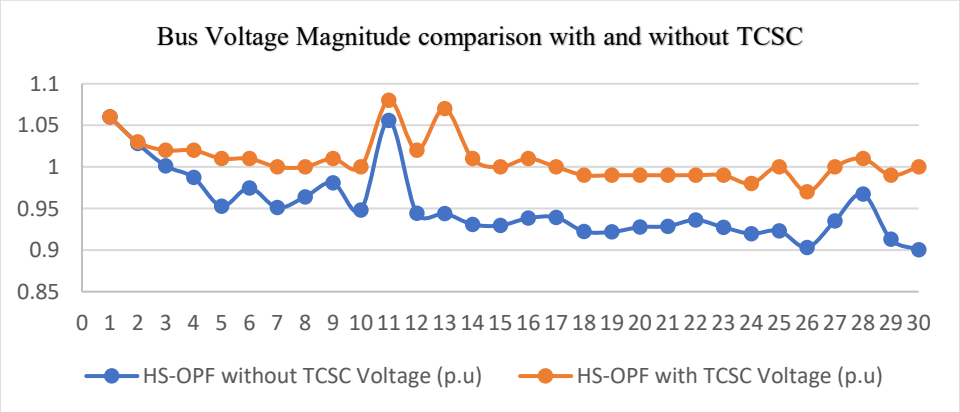

Figure.4: Bus-Wise Voltage Magnitude Comparison Using HS-OPF With and Without TCSC

The results shown in Fig.4, which compares the voltage magnitudes at each bus with and without TCSC in the HS-based OPF optimization, indicate that TCSC plays a significant role in enhancing the voltage stability of the system.

Journal of Information Systems Engineering and Management
2024, 9(4s)
e-ISSN: 2468-4376
https://www.jisem-journal.com/

Research Article

Buses such as Bus 5, Bus 18, and Bus 19 experience a notable increase in voltage, with values rising from 0.95289 p.u. to 1.01 p.u., 0.92247 p.u. to 0.99 p.u., and 0.9218 p.u. to 0.99 p.u., respectively. This demonstrates TCSC's effectiveness in stabilizing voltage at weaker buses, which are more prone to voltage drops under normal operating conditions. On the other hand, buses like Bus 1 (1.06 p.u.) and Bus 11 (1.05587 p.u.) exhibit no significant change, as they are already operating at optimal voltage levels. This suggests that TCSC's impact is more beneficial for buses that have lower voltage levels in the pre-contingency state. Overall, the introduction of TCSC improves the voltage profile across the network, leading to a more stable and efficient power system. These findings emphasize the value of incorporating TCSC in OPF optimization to enhance voltage stability, especially in buses that are vulnerable to voltage instability.

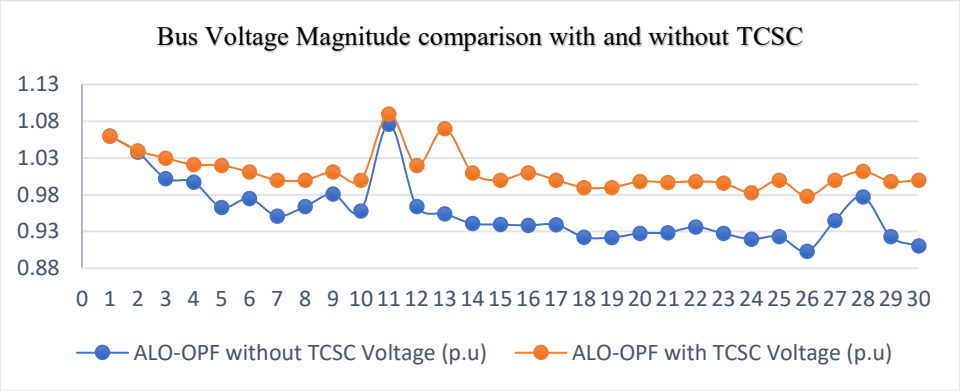

Figure.5: Bus-Wise Voltage Magnitude Comparison Using ALO-OPF With and Without TCSC

Fig.5 presents a comprehensive comparison of bus-wise voltage magnitudes derived from ALO-based OPF with and without the integration of TCSC. The data demonstrates that incorporating TCSC results in a noticeable enhancement in voltage profiles across most buses. For example, Bus 13 improves from 0.94459 p.u. to 1.0695 p.u., and Bus 30 shows a significant voltage rise from 0.90105 p.u. to 0.9995 p.u., addressing the low-voltage condition observed in the pre-contingency state. Similar trends are seen in Bus 4 (from 0.98206 to 1.0205 p.u.) and Bus 12 (from 0.94434 to 1.0285 p.u.), reinforcing TCSC's impact on enhancing stability in weak areas of the network. While high-voltage buses such as Bus 1 remain unchanged at 1.06 p.u., the consistent improvement in voltage at other buses clearly reflects the benefit of TCSC in voltage support and regulation. Overall, Fig.4 validates the effectiveness of TCSC when combined with ALO-based OPF, resulting in a more resilient and stable power system.

5.2 OPF for 9-10 (Line outage – Severity base) Contingency Condition

Table.7 presents a detailed severity ranking of line outages based on the HSI, incorporating both LUF and FVSI for the IEEE 30-bus system under HS-based OPF. The results reveal that the line outage between bus 9 and 10 ranks highest in terms of severity with an HSI value of 0.3092, indicating it poses the most critical risk to system stability. This is followed closely by the outage between bus 15 and 23 with an HSI of 0.2928, and bus 4 and 12 with 0.2669. These rankings consistently highlight lines 4–12, 9–10, and 3–4 as recurring severe lines across the LUF and FVSI metrics, pointing to their critical role in network voltage stability and load transfer. Additionally, a high LUF value of 0.4336 for line 4–6 underlines its operational stress under contingency. The presence of line 9–10 in several severe categories underlines its vulnerability and necessitates reinforcement or strategic placement of FACTS devices. This analysis aids system planners in identifying the most stressed lines under various contingencies, supporting risk-informed decision-making for improving grid resilience.

Table.8 presents the HSI-based contingency severity ranking using the ALO based OPF approach for the IEEE 30-bus system. Each contingency case is evaluated through three key vulnerability indices: LUF, FVSI, and the proposed HSI. The results indicate that line outages involving buses 9–10, 15–23, and 4–12 dominate the higher severity rankings. Notably, line 4–12 consistently appears as a severe line across all indices, indicating its critical role in system stability. In fact, for several outage scenarios, such as 15–23 and 4–6, the line 4–12 is flagged as the most vulnerable with substantial FVSI and HSI values. The line 9–10 emerges as the most critical outage in the ranking, causing severe stress on lines 3–4 and 6–10 (high LUF and FVSI), and results in the highest HSI of 0.2492 at line 4–

Journal of Information Systems Engineering and Management
2024, 9(4s)
e-ISSN: 2468-4376
https://www.jisem-journal.com/

Research Article

12. Following this, the outage of line 15–23 also significantly stresses line 4–12, suggesting that this line bears a recurring stability burden across multiple contingencies. This underscores its potential as a candidate for FACTS device deployment to improve voltage stability and overall resilience.

Further down the ranking, although the numerical differences in HSI values among contingencies become less pronounced, line 4–12 still frequently appears as the affected line, suggesting sustained vulnerability. The consistent appearance of line 4–12 in both FVSI and HSI columns reflects its heavy loading and voltage sensitivity under stressed conditions. Overall, the application of ALO in this OPF-based contingency analysis effectively identifies the most vulnerable lines, with the line 4–12 emerging as a critical segment requiring focused attention, potentially through reactive power compensation or series compensation strategies like TCSC to enhance system security and operational flexibility.

Table.9 provides a comparative analysis of the objective function parameters using the HS-OPF technique, with and without the integration of a TCSC, under the line outage contingency condition of line 9–10 in the IEEE 30-bus system. The real power output from most generators adjusts accordingly to optimize power flow and enhance system stability. A similar trend is observed under ALO: the total generation drops from 302.9102 MW (without TCSC) to 290.8656 MW (with TCSC). These results clearly highlight the beneficial impact of incorporating TCSC during contingency scenarios. The TCSC enhances load ability and voltage support by adjusting the line reactance dynamically, thus enabling more economical and reliable power system operation. The integration of TCSC, especially under stressed network conditions like a line outage, reduces overall generation costs and maintains system performance, making it a vital component in contingency-aware OPF planning.

Table.7: HSI-Based Contingency Severity Ranking using HS based OP for the IEEE 30-bus system.

Rank	Line Outage		Severe line		LUF Value	Severe Line		FVSI	Severe line		HSI
	FB	TB	FB	TB		FB	TB		FB	TB	
1	9	10	3	4	0.3589	6	10	0.4392	4	12	0.3092
2	15	23	3	4	0.3124	4	12	0.1597	9	10	0.2928
3	4	12	4	6	0.4336	9	10	0.2064	9	10	0.2669
4	28	27	3	4	0.3308	4	12	0.217	9	10	0.2426
5	4	6	4	12	0.2465	4	12	0.2302	4	12	0.2383
6	6	10	3	4	0.3155	4	12	0.178	9	10	0.2202
7	3	4	9	10	0.2497	4	12	0.1884	9	10	0.2147
8	12	15	4	6	0.3207	9	10	0.1592	9	10	0.2088
9	25	27	3	4	0.314	9	10	0.1758	9	10	0.2066
10	6	28	3	4	0.3205	4	12	0.174	9	10	0.2025
11	12	16	3	4	0.3125	4	12	0.1546	9	10	0.2022
12	15	18	3	4	0.313	4	12	0.1588	9	10	0.1996
13	12	14	3	4	0.3134	4	12	0.1603	9	10	0.1985
14	16	17	3	4	0.3124	4	12	0.1646	9	10	0.1977
15	24	25	3	4	0.3127	9	10	0.3689	9	10	0.1976
16	18	19	3	4	0.3126	4	12	0.162	9	10	0.197
17	27	30	3	4	0.3152	4	12	0.1648	9	10	0.1969
18	6	7	3	4	0.2766	4	12	0.154	9	10	0.1967
19	27	29	3	4	0.3146	4	12	0.1641	9	10	0.1966
20	14	15	3	4	0.3127	4	12	0.1621	9	10	0.1961
21	29	30	3	4	0.3133	4	12	0.163	9	10	0.1961
22	10	21	3	4	0.3189	4	12	0.2095	4	12	0.1953
23	23	24	4	6	0.2592	4	12	0.1595	9	10	0.1949
24	21	23	3	4	0.3128	4	12	0.1691	9	10	0.1933
25	6	9	3	4	0.3157	9	10	0.1696	9	10	0.1932

Journal of Information Systems Engineering and Management
2024, 9(4s)
e-ISSN: 2468-4376
https://www.jisem-journal.com/

Research Article

26	19	20	3	4	0.3144	4	12	0.1806	9	10	0.1918
27	10	22	3	4	0.3135	4	12	0.1634	9	10	0.1918
28	22	24	3	4	0.3135	4	12	0.1634	9	10	0.1918
29	10	20	3	4	0.3155	4	12	0.1864	9	10	0.1913
30	10	17	3	4	0.3144	4	12	0.2034	4	12	0.1883

FB – From Bus **TB** – To Bus

Table.10 presents a comparative summary of the total power generation, losses, voltage deviation, and fuel cost using HS and ALO based OPF strategies, both excluding and including the TCSC under the 9–10 line outage contingency in the IEEE 30-bus system. Without TCSC, the HS algorithm results in a total real power generation of 303.4872 MW, with corresponding real and reactive power losses of 20.0872 MW and 38.6 MVAR, respectively. Voltage deviation stands at 2.9517 p.u., and the fuel cost is $1379.6/hr. With the integration of TCSC, these parameters improve significantly: real power generation reduces to 299.5843 MW, losses drop to 16.1843 MW and 20.53 MVAR, voltage deviation declines to 1.2327 p.u., and the fuel cost falls to $1297.3/hr.

A similar improvement trend is observed in the ALO results. Without TCSC, the total generation is 302.9102 MW with 19.5102 MW of real power loss, 22.47 MVAR of reactive power loss, a voltage deviation of 1.4023 p.u., and a fuel cost of $1359.2/hr. When TCSC is introduced, total generation drops notably to 290.8656 MW, real and reactive losses fall to 7.4656 MW and 15.42 MVAR, voltage deviation decreases to 0.8132 p.u., and the fuel cost lowers to $1274.5/hr. These results clearly demonstrate the effectiveness of incorporating TCSC in OPF strategies. The TCSC not only enhances the system's efficiency by minimizing losses and voltage deviations but also significantly reduces operational costs, especially during contingency scenarios.

Table.8:HSI-Based Contingency Severity Ranking using ALO based OP for the IEEE 30-bus system.

Rank	Line Outage		Severe line		LUF Value	Severe Line		FVSI	Severe line		HSI
	FB	TB	FB	TB		FB	TB		FB	TB	
1	9	10	3	4	0.2989	6	10	0.3792	4	12	0.2492
2	15	23	3	4	0.2524	4	12	0.0997	9	10	0.2328
3	4	12	4	6	0.3736	9	10	0.1464	9	10	0.2069
4	28	27	3	4	0.2708	4	12	0.157	9	10	0.1826
5	4	6	4	12	0.1865	4	12	0.1702	4	12	0.1783
6	6	10	3	4	0.2555	4	12	0.118	9	10	0.1602
7	3	4	9	10	0.1897	4	12	0.1284	9	10	0.1547
8	12	15	4	6	0.2607	9	10	0.0992	9	10	0.1488
9	25	27	3	4	0.254	9	10	0.1158	9	10	0.1466
10	6	28	3	4	0.2605	4	12	0.114	9	10	0.1425
11	12	16	3	4	0.2525	4	12	0.0946	9	10	0.1422
12	15	18	3	4	0.253	4	12	0.0988	9	10	0.1396
13	12	14	3	4	0.2534	4	12	0.1003	9	10	0.1385
14	16	17	3	4	0.2524	4	12	0.1046	9	10	0.1377
15	24	25	3	4	0.2527	9	10	0.3089	9	10	0.1376
16	18	19	3	4	0.2526	4	12	0.102	9	10	0.137
17	27	30	3	4	0.2552	4	12	0.1048	9	10	0.1369
18	6	7	3	4	0.2166	4	12	0.094	9	10	0.1367
19	27	29	3	4	0.2546	4	12	0.1041	9	10	0.1366
20	14	15	3	4	0.2527	4	12	0.1021	9	10	0.1361
21	29	30	3	4	0.2533	4	12	0.103	9	10	0.1361
22	10	21	3	4	0.2589	4	12	0.1495	4	12	0.1353
23	23	24	4	6	0.1992	4	12	0.0995	9	10	0.1349

Journal of Information Systems Engineering and Management
2024, 9(4s)
e-ISSN: 2468-4376
https://www.jisem-journal.com/

Research Article

24	21	23	3	4	0.2528	4	12	0.1091	9	10	0.1333
25	6	9	3	4	0.2557	9	10	0.1096	9	10	0.1332
26	19	20	3	4	0.2544	4	12	0.1206	9	10	0.1318
27	10	22	3	4	0.2535	4	12	0.1034	9	10	0.1318
28	22	24	3	4	0.2535	4	12	0.1034	9	10	0.1318
29	10	20	3	4	0.2555	4	12	0.1264	9	10	0.1313
30	10	17	3	4	0.2544	4	12	0.1434	4	12	0.1283

FB – From Bus **TB** – To Bus

Table.9: Contrast of objective function parameters employing HS-OPF excluding and including TCSC for 9-10 (Line outage) Contingency Condition

Method	PG1 (MW)	PG2 (MW)	PG5 (MW)	PG8 (MW)	PG11 (MW)	PG13 (MW)	Total Generation (MW)	TCSC Rating (P.U)
HS without TCSC	136.6123	35.3976	31.1769	43.8011	46.5213	9.978	303.4872	---------
HS with TCSC at Line No 4-12	134.9623	34.3818	32.3027	44.4478	43.4897	10	299.5843	P_{tcsc}=0.4842 Q_{tcsc}=0.0124 X=0.02
ALO without TCSC	133.3714	22.3396	26.8427	29.9887	80.5158	9.852	302.9102	---------
ALO with TCSC at Line No 4-12	133.1793	20.1007	26.4235	22.3394	78.8227	10	290.8656	P_{tcsc}=0.4832 Q_{tcsc}=0.0122 X=0.02

Table.10: Total Power Generation and Losses

Parameter	HS without TCSC	HS with TCSC at Line No 4-12	ALO without TCSC	ALO with TCSC at Line No 4-12
Total Real Power (MW)	303.4872	299.5843	302.9102	290.8656
Real Power Loss (MW)	20.0872	16.1843	19.5102	7.4656
Reactive Power Loss (MVAR)	38.6	20.53	22.47	15.42
Voltage Deviation (p.u.)	2.9517	1.2327	1.4023	0.8132
Fuel Cost ($/hr)	1379.6	1297.3	1359.2	1274.5

Journal of Information Systems Engineering and Management
2024, 9(4s)
e-ISSN: 2468-4376
https://www.jisem-journal.com/

Research Article

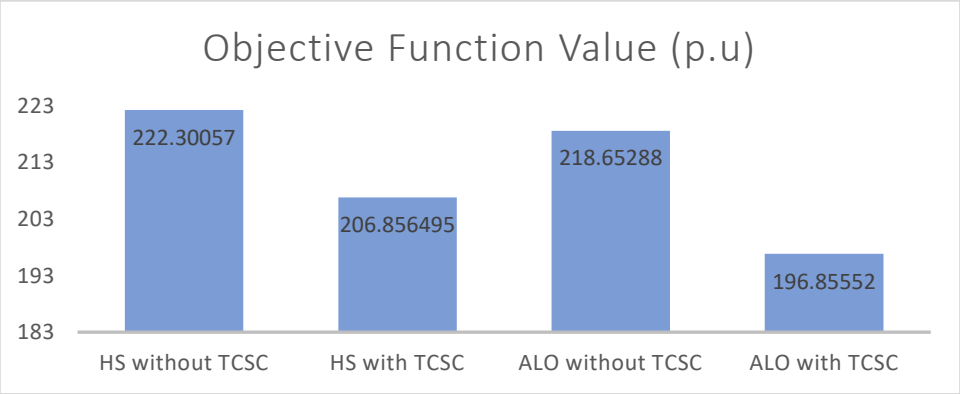

Figure.5: Objective Function (F) Comparison for HS and ALO Algorithms with and Without TCSC

The objective function values for the HS and ALO algorithms, both with and without TCSC, are compared as follows. For the HS algorithm without TCSC, the objective function value is 222.30057 p.u. When TCSC is included, the objective function value decreases to 206.856495 p.u. Similarly, for the ALO algorithm without TCSC, the value stands at 218.65288 p.u., while with TCSC, the objective function value reduces to 196.85552 p.u. These results indicate that the inclusion of TCSC in both algorithms leads to a reduction in the objective function values, suggesting improved system performance in terms of minimizing the overall objective.

Table.11 presents the bus voltage magnitudes in the pre- and post-contingency states for the HS algorithm-based OPF with and without TCSC. The values are given in per unit (p.u.) for each bus number. In the pre-contingency state, the voltage magnitudes for all buses are within the acceptable range, showing stability across the system. For instance, at Bus 1, the voltage remains at 1.06 p.u. in both scenarios (with and without TCSC). However, when a contingency occurs, the voltage magnitudes for some buses decrease in the case without TCSC, whereas the inclusion of TCSC helps in improving the voltage levels. For example, Bus 16's voltage drops from 0.93834 p.u. to 0.8837 p.u. without TCSC but increases to 1.01 p.u. post-contingency when TCSC is employed. Similarly, at Bus 14, without TCSC, the voltage decreases from 0.93095 p.u. to 0.8802 p.u., while with TCSC, the voltage maintains stability at 1.0095 p.u. These results suggest that TCSC aids in voltage stabilization during contingencies, enhancing the performance of the power system by mitigating the voltage dips that occur under fault conditions. The overall benefit of using TCSC in the HS-based OPF is evident across multiple buses, with voltage levels showing improvement, particularly in more critical buses.

Table.11: Bus voltage magnitudes in pre & post contingency state in Harmony Search algorithm based OPF without & with TCSC

Bus No	Pre-Contingency Voltage (p.u.)		Post-Contingency Voltage (p.u.)		Bus No	Pre-Contingency Voltage (p.u.)		Post-Contingency Voltage (p.u.)	
	HS-based OPF without TCSC	HS-based OPF with TCSC	HS-based OPF without TCSC	HS-based OPF with TCSC		HS-based OPF without TCSC	HS-based OPF with TCSC	HS-based OPF without TCSC	HS-based OPF with TCSC
1	1.06	1.06	1.06	1.06	16	0.93834	1.01	0.8837	1.0095
2	1.02812	1.03	1.006	1.0395	17	0.93935	1	0.8789	0.9995
3	1.00123	1.02	0.9746	1.0295	18	0.92247	0.99	0.8628	0.9895
4	0.98731	1.02	0.9553	1.0195	19	0.9218	0.99	0.8606	0.9895
5	0.95289	1.01	0.9164	1.0095	20	0.92758	0.99	0.8668	0.9895
6	0.97485	1.01	0.9396	1.0095	21	0.92863	0.99	0.8605	0.9895
7	0.95112	1	0.915	0.9995	22	0.93617	0.99	0.856	0.9995
8	0.96394	1	0.9279	1.0095	23	0.92741	0.99	0.8569	0.9895

Journal of Information Systems Engineering and Management
2024, 9(4s)
e-ISSN: 2468-4376
https://www.jisem-journal.com/

Research Article

9	0.98105	1.01	0.9316	1.0195	24	0.91964	0.98	0.8136	0.9795
10	0.94802	1	0.8867	0.9995	25	0.92319	1	0.7337	0.9895
11	1.05587	1.08	1.0134	1.0795	26	0.90326	0.97	0.7086	0.9695
12	0.94418	1.02	0.8986	1.0295	27	0.93521	1	0.6992	1.0095
13	0.94409	1.07	0.8987	1.0695	28	0.96742	1.01	0.9397	1.0095
14	0.93095	1.01	0.8802	1.0095	29	0.91321	0.99	0.6686	0.9895
15	0.92958	1	0.8731	0.9995	30	0.90055	1	0.6504	0.9995

Table.12: Bus voltage magnitudes in pre & post contingency state in ALO algorithm based OPF without & with TCSC

Bus No	Pre-Contingency Voltage (p.u.)		Post-Contingency Voltage (p.u.)		Bus No	Pre-Contingency Voltage (p.u.)		Post-Contingency Voltage (p.u.)	
	ALO-based OPF without TCSC	ALO - based OPF with TCSC	ALO-based OPF without TCSC	ALO - based OPF with TCSC		ALO-based OPF without TCSC	ALO - based OPF with TCSC	ALO-based OPF without TCSC	ALO - based OPF with TCSC
1	1.06	1.06	1.06	1.06	16	0.93591	1.0115	0.8891	1.0115
2	1.02481	1.0415	1.0094	1.0415	17	0.93707	0.9995	0.8835	0.9995
3	0.99842	1.0305	0.9797	1.0305	18	0.92153	0.9895	0.8687	0.9895
4	0.98206	1.0205	0.9609	1.0205	19	0.92077	0.9895	0.8658	0.9895
5	0.95339	1.011	0.9211	1.011	20	0.92667	0.9895	0.871	0.9895
6	0.97468	1.0105	0.9448	1.0105	21	0.92784	0.9895	0.8656	0.9895
7	0.95103	1.001	0.9195	1.001	22	0.93497	0.9995	0.8605	0.9995
8	0.96311	1.0095	0.9326	1.0095	23	0.92652	0.9895	0.8617	0.9895
9	0.97892	1.0215	0.9357	1.0215	24	0.91914	0.9795	0.8181	0.9795
10	0.94683	1.0015	0.8917	1.0015	25	0.92262	0.9895	0.7385	0.9895
11	1.05371	1.0795	1.0181	1.0795	26	0.90426	0.9695	0.7137	0.9695
12	0.94434	1.0285	0.903	1.0285	27	0.93471	1.0095	0.7041	1.0095
13	0.94459	1.0695	0.9025	1.0695	28	0.96687	1.0095	0.9435	1.0095
14	0.93033	1.0115	0.8854	1.0115	29	0.91332	0.9895	0.6734	0.9895
15	0.92694	1.0005	0.8787	1.0005	30	0.90105	0.9995	0.6557	0.9995

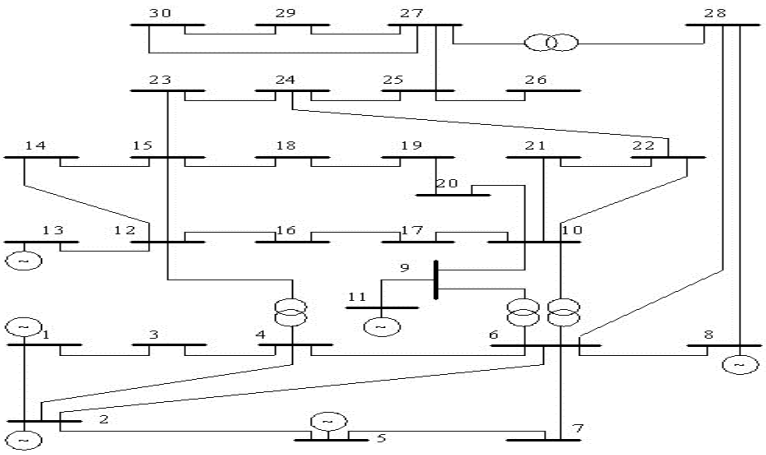

Figure.6: IEEE 30 Bus system Line Diagram

Table.12 presents the bus voltage magnitudes in the pre- and post-contingency states for the ALO algorithm-based OPF with and without TCSC. The values are given in per unit (p.u.) for each bus number. In the pre-contingency state, the voltage magnitudes for all buses are generally stable in both scenarios. For instance, at Bus 1, the voltage remains constant at 1.06 p.u. in both cases (with and without TCSC). However, when a contingency occurs, the voltage magnitudes for several buses show a significant improvement when TCSC is included, indicating better system stability during disturbances.

For example, at Bus 16, the voltage drops from 0.93591 p.u. to 0.8891 p.u. without TCSC, but with TCSC, it increases to 1.0115 p.u. Similarly, Bus 14 shows an improvement from 0.93033 p.u. to 0.8854 p.u. without TCSC, while with TCSC, the voltage remains stable at 1.0115 p.u. These results highlight the beneficial effect of incorporating TCSC into the ALO-based OPF, as it helps maintain or restore voltage stability across the network after a contingency event. The use of TCSC in the ALO-based OPF algorithm enhances the voltage recovery and helps in minimizing voltage dips that occur at critical buses during contingency scenarios. This shows the effectiveness of TCSC in improving the system's voltage profile, especially under fault conditions.

6. CONCLUSION

Under contingency especially, maintaining operational dependability and system stability remains a major difficulty in contemporary power systems. Minimising generating cost, transmission losses, and voltage variations helps to guarantee the effective use of system resources by means of OPF Especially the TCSC, the integration of FACTS devices has shown great potential in improving voltage stability and reducing the negative consequences of system contingency. This work proposes a complete OPF framework using a HSI, developed by aggregating the FVSI with the LUF, to find and rank important transmission lines under stressed system conditions. Simultaneously, generator output is optimized with the ALO, a strong metaheuristic method well-known for high convergence speed and great global search capability. System vulnerabilities were assessed using conventional contingency analysis methods, which also helped to direct the best location of TCSC devices. Results of simulation on the IEEE 30-bus test system confirm the efficiency of the suggested method. In contingency conditions, the combined approach greatly increases voltage profiles, lowers power losses, and increases general operational efficiency. A practical and high-performance way to improve the resilience and dependability of developing power systems is provided by the shown synergy between HSI-guided TCSC allocation and ALO-based generator adjustment. For real-time applications in smart grids, where sustainable power system management depends on stability, adaptability, and optimality, this paradigm has potential.

REFERENCES

[1] Paul Charles; Fateh Mehazzem; Ted Soubdhan “A Review on Optimal Power Flow Problems: Conventional and Metaheuristic Solutions” 2020 2nd International Conference on Smart Power & Internet Energy Systems (SPIES) DOI: 10.1109/SPIES48661.2020.9242994
[2] Jeremy Lin; Fernando H. Magnago “Optimal Power Flow” Publisher: Wiley-IEEE Press DOI: 10.1002/9781119179382.ch6
[3] Qing-Hua Wu; Anjan Bose; Chanan Singh; Joe H. Chow; Gang Mu; Yuanzhang Sun “Control and Stability of Large-scale Power System with Highly Distributed Renewable Energy Generation: Viewpoints from Six Aspects” Publisher: CSEE DOI: 10.17775/CSEEJPES.2022.08740
[4] F. Gao [a 1], G.B. Sheble [b 2] “Electricity market equilibrium model with resource constraint and transmission congestion” Electric Power Systems Research Volume 80, Issue 1, January 2010, Pages 9-18 doi.org/10.1016/j.epsr.2009.07.007
[5] J.L. Carpentier “Optimal Power Flows: Uses, Methods and Developments” IFAC Proceedings Volumes
[6] Volume 18, Issue 7, July 1985, Pages 11-21 doi.org/10.1016/S1474-6670(17)60410-5
[7] Sajan Varma “FACTS devices for stability enhancements” 2015 International Conference on Green Computing and Internet of Things (ICGCIoT) DOI: 10.1109/ICGCIoT.2015.7380430
[8] Mehmet Yesilbudak; Salih Ermis; Ramazan Bayindir Investigation of the effects of FACTS devices on the voltage stability of power systems 2017 IEEE 6th International Conference on Renewable Energy Research and Applications (ICRERA) 10.1109/ICRERA.2017.8191222

[9] Sai Ram Inkollu [a], Venkata Reddy Kota [b] "Optimal setting of FACTS devices for voltage stability improvement using PSO adaptive GSA hybrid algorithm" Engineering Science and Technology, an International Journal Volume 19, Issue 3, September 2016, Pages 1166-1176.
[10] doi.org/10.1016/j.jestch.2016.01.011
[11] Hingorani G, Gyugyi I. Understanding FACTS: Concepts and technology of Flexible AC Transmission Systems. New York: IEEE Press, 2000. Understanding FACTS: Concepts and Technology of Flexible AC Transmission Systems | IEEE eBooks | IEEE Xplore
[12] Mathur RM, Varma RK. Thyristor-based FACTS controllers for electrical transmission systems. Piscataway: IEEE Press, 2002. Thyristor-Based FACTS Controllers for Electrical Transmission Systems | IEEE eBooks | IEEE Xplore
[13] Mondal D, Chakrabarti A, Sengupta A. Optimal placement and parameter setting of SVC and TCSC using PSO to mitigate small signal stability problem. Int J Electr Power Energ Syst 2012; 42(1): 334-40.
[14] doi.org/10.1016/j.ijepes.2012.04.017
[15] Idris RM, Khairuddin A, Mustafa MW. Optimal allocation of FACTS devices for ATC enhancement using Bees algorithm. World Acad Sci Eng Technol 2009; 3(6): 313-20. Optimal choice of FACTS devices for ATC enhancement using Bees Algorithm | IEEE Conference Publication | IEEE Xplore
[16] Tripathy M, Mishra S. Bacteria foraging based solution to optimize both real power loss and voltage stability limit. IEEE Trans Power Syst 2007; 22(1): 240-8. 10.1109/TPWRS.2006.887968
[17] Rajasekaran S, Muralidharan S. Firefly algorithm in determining maximum load utilization point and its enhancement through opti mal placement of FACTS device. Circuit Syst 2016; 7: 3081-94. 10.4236/cs.2016.710262
[18] Rakesh Roshan; Padarbinda Samal; Pampa Sinha Optimal placement of FACTS devices in power transmission network using power stability index and fast voltage stability index 14-15 February 2020 10.1109/ICE348803.2020.9122975
[19] Hadi K, Hamid A. Voltage stability improvement by using FACTS elements with economic consideration. Ciênc Nat 2015; 37(2): 162-7. Zhao, Y., & Wang, Y. (2005). Optimal power flow based on Genetic Algorithms. *IEEE Transactions on Power Systems*, 20(4), 1819-1826.
[20] https://doi.org/10.5902/2179460X20767
[21] Virginijus Radziukynas & Ingrida Radziukyniene Optimization Methods Application to Optimal Power Flow in Electric Power Systems Chapter pp 409–436 Optimization Methods Application to Optimal Power Flow in Electric Power Systems | SpringerLink
[22] Mohamed Ebeed , Salah Kamel , Francisco Jurado Chapter 7 - Optimal Power Flow Using Recent Optimization Techniques Classical and Recent Aspects of Power System Optimization 2018, Pages 157-183 doi.org/10.1016/B978-0-12-812441-3.00007-0
[23] Kiran Kumar Kuthadi, N D. Sridhar & C. H. Ravi Kumar Optimal placement of FACTs devices for enhancing of transmission system performance using whale optimization algorithm 20 June 2022 Optimal placement of FACTs devices for enhancing of transmission system performance using whale optimization algorithm | International Journal on Interactive Design and Manufacturing (IJIDeM)
[24] Debasish Choudhury; Sarmila Patra Multi objective optimal power flow using particle swarm optimization technique 03-05 October 2016 2016 International Conference on Signal Processing, Communication, Power and Embedded System (SCOPES) 10.1109/SCOPES.2016.7955644
[25] Maysam Abbasi, Ehsan Abbasi & Behnam Mohammadi-Ivatloo Single and multi-objective optimal power flow using a new differential-based harmony search algorithm 18 May 2020 Single and multi-objective optimal power flow using a new differential-based harmony search algorithm | Journal of Ambient Intelligence and Humanized Computing
[26] Souhil Mouassa , Tarek Bouktir , Ahmed. Salhi Ant lion optimizer for solving optimal reactive power dispatch problem in power systems Engineering Science and Technology, an International Journal Volume 20, Issue 3, June 2017, Pages 885-895 doi.org/10.1016/j.jestch.2017.03.006
[27] Seyedali Mirjalili The Ant Lion Optimizer Advances in Engineering Software Volume 83, May 2015, Pages 80-98 doi.org/10.1016/j.advengsoft.2015.01.010

Journal of Information Systems Engineering and Management
2024, 9(4s)
e-ISSN: 2468-4376
https://www.jisem-journal.com/

Research Article

[28] Laith Abualigah, Mohammad Shehab, Mohammad Alshinwan, Seyedali Mirjalili & Mohamed Abd Elaziz Ant Lion Optimizer: A Comprehensive Survey of Its Variants and Applications 03 April 2020 Ant Lion Optimizer: A Comprehensive Survey of Its Variants and Applications | Archives of Computational Methods in Engineering
[29] Yue Song; Tao Liu; Yunhe Hou Voltage Stability Constrained Optimal Power Flow Considering PV-PQ Bus Type Switching: Formulation and Convexification IEEE Transactions on Power Systems (Volume: 39, Issue: 2, March 2024) 3336 – 3348 10.1109/TPWRS.2023.3313656
[30] D. Gan; R.J. Thomas; R.D. Zimmerman Stability-constrained optimal power flow IEEE Transactions on Power Systems (Volume: 15, Issue: 2, May 2000) 535 – 540 10.1109/59.867137
[31] Amr Adel Mohamed, Bala Venkatesh Voltage stability constrained line-wise optimal power flow29 March 2019 https://doi.org/10.1049/iet-gtd.2018.5452
[32] Dugan, R. C., & McGranaghan, M. F. (2002). Electrical Power Systems Quality. *McGraw-Hill*, New York. Electrical Power Systems Quality, Third Edition - Roger C. Dugan, Mark F. McGranaghan, Surya Santoso, H. Wayne Beaty - Google Books
[33] Mehebub Alam Determination of Power System Contingency Ranking Using Novel Indices 14 February 2022 Determination of Power System Contingency Ranking Using Novel Indices | SpringerLink
[34] Saurabh Ratra, Rajive Tiwari, K.R. Niazi Voltage stability assessment in power systems using line voltage stability index Computers & Electrical Engineering Volume 70, August 2018, Pages 199-211 doi.org/10.1016/j.compeleceng.2017.12.046